

# **Strain analysis of Archean rocks from the Virginia Horn area, NE Minnesota**

Ben Christensen  
Undergraduate Thesis under Jim Welsh  
Gustavus Adolphus College Geology

## **Abstract**

The Virginia Horn refers to the structure where the outcrop pattern of the Biwabik Iron Formation makes a sharp bend southward and then back north as a part of a broad, gently plunging anticlinal and synclinal flexure, near the city of Virginia in northeastern Minnesota, exposing supracrustal rocks of Archean age within the core of the anticline. Three deformation events have affected these rocks (Jirsa and Boerboom 2003). Strain analysis on three graywacke samples from the area was performed in order to determine whether the small-scale structures present in the rocks are consistent with the megascopic structure. Specifically, the  $R_f/\Phi$  method proved to be reliable and consistent when applied to these samples. The strain data show that graywackes from the area exhibit a degree of flattening consistent with the  $D_2$  deformation.

### **Acknowledgements**

I would like to thank Jim Welsh for his assistance and advisement throughout this project. Also Laura Triplett and Alan Gishlick for their help with writing this thesis. And Alan again for all his technological help throughout the year.

## Table of Contents

### Introduction

Purpose.....	1
Geologic Setting.....	1
Previous Work.....	3

### Methods

Sample Collection.....	5
Strain Analysis.....	6

Results.....	9
--------------	---

Discussion.....	14
-----------------	----

Future Work.....	15
------------------	----

Conclusion.....	16
-----------------	----

Appendix I.....	16
-----------------	----

Appendix II.....	19-20
------------------	-------

References.....	21
-----------------	----

## **Introduction**

A complexly deformed sequence of Archean supracrustal metavolcanic and metasedimentary rocks and minor felsic intrusions are exposed in the core of a broad anticlinal flexure in the Biwabik Iron Formation of northeastern Minnesota referred to as the “Virginia Horn” (Figure 1, Welsh et al., 1989; Jirsa and Boerboom, 2003). At least three episodes of deformation have affected these rocks, and a major fault/shear complex cuts through them (Welsh, 1989; Jirsa and Boerboom, 2003). Jirsa and Boerboom (2003) detail the structural history of this area. The purpose of this study is to attempt strain analysis in order to further document the strain history of these rocks.

## **Geologic Setting**

The Archean rocks of northeastern Minnesota, including those exposed within the Virginia Horn, are considered to be an extension of the Wawa Subprovince of the Superior Province (Jirsa and Boerboom, 2003). The supracrustal rocks specific to the Virginia Horn have been intruded by the Giants Range Batholith directly to the north, and are separated by it from similar rocks in the Vermilion district to the north. Unconformably overlying this complex of Archean rocks are the sedimentary rocks of the Animikie Group, which include the Biwabik Iron Formation.

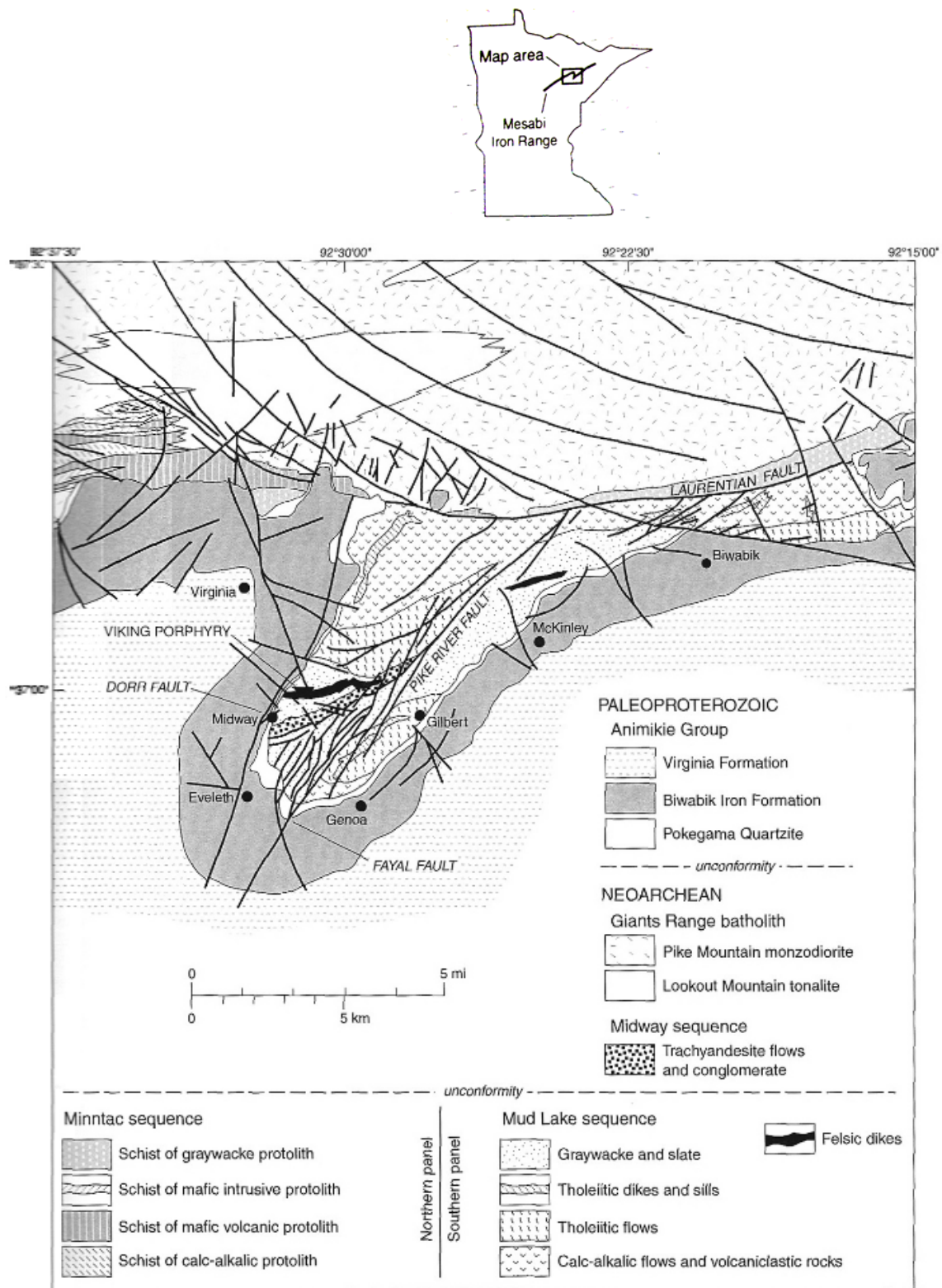


Figure 1. Map of the Virginia Horn in northeastern Minnesota

## **Previous Work**

The first detailed study of the area was done by Sutton (1963). As an extension of earlier work along the Laurentian Divide, J. Welsh began a detailed mapping project in the Virginia Horn, where he began to work out the detailed structural geology, and identified the Pike River Fault (Welsh 1989, Welsh et al., 1989; Welsh et al., 1991). Jirsa and Boerboom (1998, 2003) produced a detailed geologic map of the area, and summarized the geology in detail. They divided the rocks of the area into three groups: the Minntac, Mud Lake, and Midway sequences.

The Minntac sequence of rocks is composed mainly of schists of volcanic and sedimentary origin, which have been metamorphosed to middle amphibolite grade. It occurs in the northwestern part of the area where it is intruded by the Giants Range Batholith.

The Mud Lake sequence is believed to be of similar age to the Minntac sequence, though it experienced lower grade metamorphism, ranging from prehnite-pumpellyite to chlorite greenschist facies. This group consists of northern and southern suites of metavolcanics, separated by a main body of graywacke and slate. The graywackes are turbidites with thin layers commonly graded, and fine- to medium-sized grains with planar-laminated bedding.

The Midway sequence is embedded within the Mud Lake sequence and consists predominantly of conglomerates interlayered with a few trachyandesite flows that are fault bounded with the other Mud Lake sequence rocks. The conglomerates are composed of rocks from the Mud Lake sequence, indicating it formed after this sequence. The Mud Lake and Midway sequences were intruded by a gold-bearing quartz-feldspar porphyry named the Viking Porphyry.

Jirsa and Boerboom (2003) describe three deformation events that affected these rocks.  $D_1$  deformation involved folding, but very little metamorphism. A large syncline that folded the rocks of the Mud Lake sequence is interpreted to have formed during this event (Figure 2), and is believed to have formed concurrently with deposition, tilting these rocks to a near vertical orientation.  $D_2$  is characterized by isoclinal folding with a steeply plunging axis, accompanied by regional metamorphism. A prominent cleavage,  $S_2$ , formed during this event.  $D_3$  consists primarily of later faults in the area.

Of special significance is the Pike River Fault system, trending almost along the fold axis of the Virginia Horn. Rocks along this fault exhibit ductile shear and are very phyllonitized. Map patterns and rock formations suggest mainly sinistral movement (Welsh et al, 1991, Jirsa and Boerboom 2003). Jirsa and Boerboom (2003) suggest that this movement initiated during  $D_1$  deformation, before the formation of the Mud Lake Syncline. Pull apart structures then developed and were concurrently filled by the conglomerates and flows of the Midway sequence; however, later kinematic indicators (such as minor folds) show dextral movement of the fault, suggesting reactivation of the fault in a later stage of deformation (Welsh et al, 1989; Jirsa and Boerboom, 2003). Jirsa and Boerboom did not, however, attribute this dextral movement to any specific deformational event. Welsh (pers.comm.) thinks that this later reactivation might be Penokean. This combination of faulting and direction change could be a possible factor in the formation of the overall Virginia Horn structure (Welsh pers.comm).



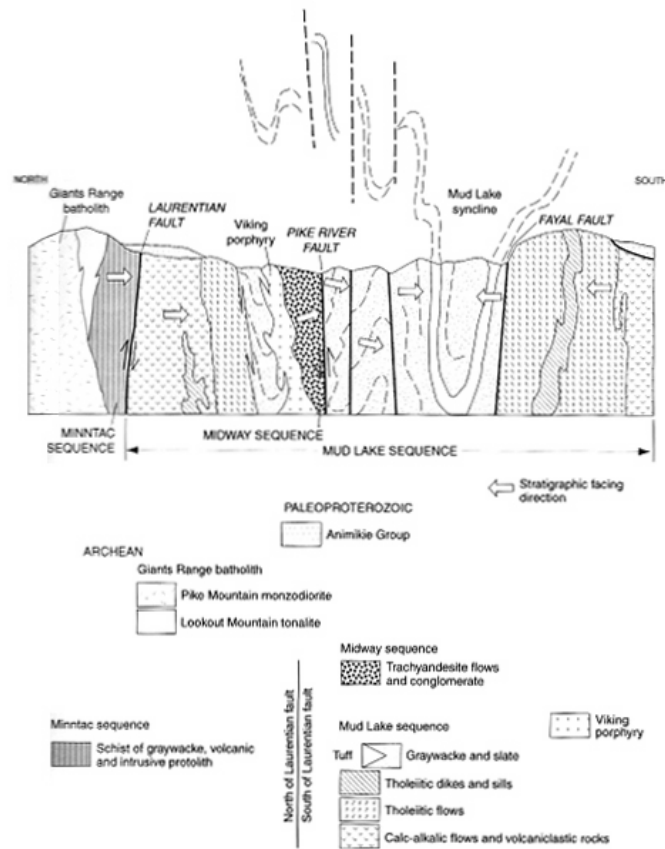


Figure 2. Cross section of the Virginia Horn showing locations of the three named sequences by Jirsa and Boerboom (2003)

## Methods

### *Sample Collection*

Oriented samples from the Horn area were collected during previous fieldwork by J. Welsh. These include graywackes from the Mud Lake sequence. All samples were oriented with respect to the  $S_2$  prominent foliation. For each sample faces were cut and labeled A, B and C. A and B lie perpendicular to  $S_2$  with face A cut essentially in the horizontal plane, and face B essentially in the vertical plane; face C lies in the plane of foliation (see figure 3).

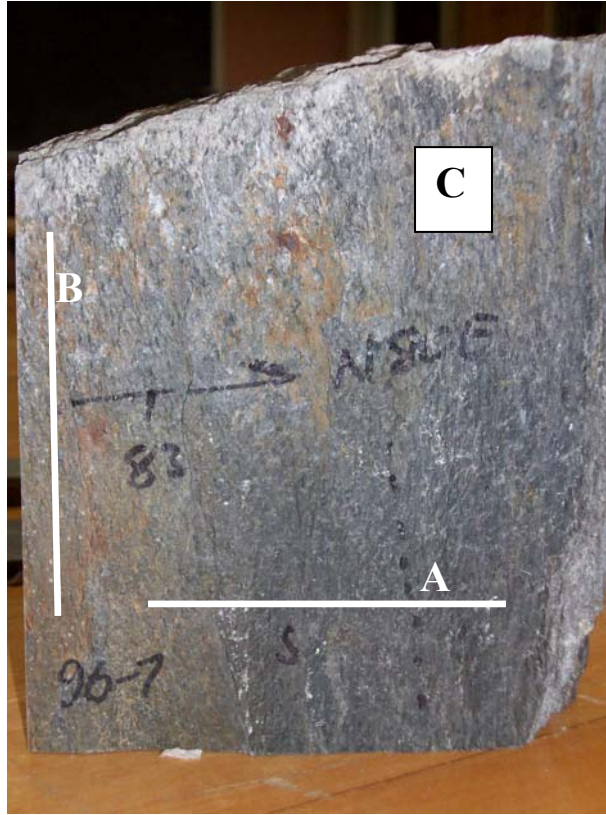


Figure 3. Example of an oriented greywacke from the Mud Lake Sequence. The white lines indicate direction of faces A and B, with face C lying within the plane of the rock-face.

### *Strain Analysis*

The  $R_f/\Phi$  method was used to assess the strain character of these rocks. The method, developed by Ramsay (1967) and Dunnet (1969), and later modified by Lisle (1985), can be used to provide reasonably consistent strain data from this area. The method provides a way to achieve the finite strain ellipse of a rock body using objects that were not originally circular (i.e. elliptical) and show no original fabric. It is based on measuring the axial ratio of the final strain ellipse of an object ( $R_f$ ) and the angle between the long axis of the strain ellipse and the trace of foliation ( $\Phi$ ), which is  $S_2$  for these samples. These can be compared to the original axial ratios and angular orientations for the object ( $R_i$  and theta,  $\Theta$ , respectively), and used to determine the axial ratio for the strain ellipse of the entire rock sample ( $R_s$ ).

Three graywacke samples, 6, 7, and 11, were chosen for this test because of more obvious signs of deformation, such as prominent  $S_2$  cleavage. Quartz grains were chosen due to more distinguishable grain boundaries and a more likely chance that dissolution or mass change of the grain had not occurred. Using a Motic Images 3100 digital microscope camera and software, grains were measured for  $R_f$  values. Forty grains per section were measured for long and short axes of each grain's projected strain ellipse, along with the angle  $\phi$  ( $\Phi$ ).

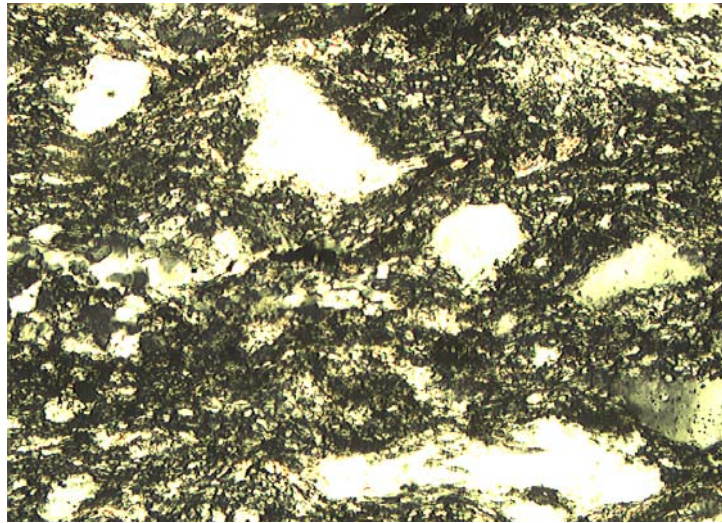


Figure 4. Example of a thin section from sample 6, section B.  $R_f$  and  $\Phi$  data were obtained from visible quartz grains. The direction of foliation is straight across the slide.

Once all data had been collected  $I_{\text{sym}}$  tests were performed to assure that the data is consistent with the original assumption that no previous fabric was present in the rock. This test consists of determining the harmonic mean of the  $R_f$  values and the vector mean of  $\Phi$  values, and by plotting them as lines with the  $R_f$  versus  $\Phi$  data. When the two means are graphed as lines, they produce four quadrants within the plot.  $I_{\text{sym}}$  is a function of the number of data points in each quadrant (for more information see Lisle, 1985). The values of  $I_{\text{sym}}$  are then compared to critical values from the literature as presented in Table 1. For an  $I_{\text{sym}}$  value higher than the critical value for the sample size and projected  $R_s$  value the sample can be considered to have contained no original fabric. If a previous fabric were present, the

final  $R_s$  value would be a measure of the strain on that fabric, and not of the original host rock, and indicate need of further testing and manipulation in order to achieve a clear history of the deformation of the original host rock.

Table 1. Critical  $I_{sym}$  values as taken from Lisle (1985). These values are based on a 95% confidence interval, and are based on both sample size and projected  $R_f$  values based on the harmonic mean of the data, which tends to slightly overshoot the  $R_s$  value.

	Sample Size Number of grains				
$R_s$	20	30	40	100	200
1.5	0.3	0.51	0.6	0.74	0.82
2	0.5	0.63	0.73	0.8	0.86
3	0.5	0.63	0.73	0.8	0.87
5	0.5	0.63	0.73	0.82	0.87
10	0.6	0.63	0.73	0.82	0.87

If samples fit this original assumption, the plots can then be overlain with  $R_s$  value plots, as provided by Lisle (1985). An example is shown in Figure 5. The appropriate  $R_s$  value is selected from the overlay that shows the best fit. From this plot the strain ellipse ratio ( $R_s$ ), original axis ratios ( $R_i$ ), and orientations ( $\Theta$ ) for the rock sample can be determined.

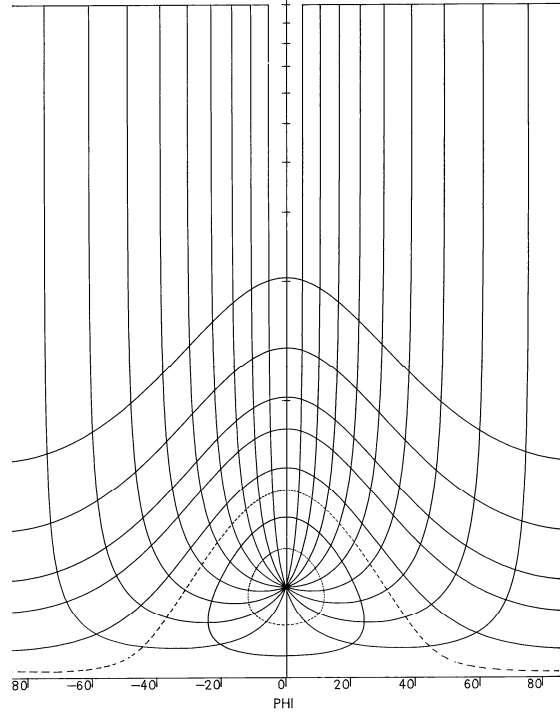


Figure 5. Example  $R_s$  plot. This represents a finite strain ratio of 1.7. Plotted points ( $R_F$  vs.  $\Phi$ ) are matched to the  $R_i$  and theta curves on the chart.

The resulting  $R_s$  values for each sample were then compared to determine if the results are consistent. Upon discovering this was the case all data were plotted together to determine an average  $R_s$ .

## Results

Symmetry data for the curves are presented in Table 2. These values are higher than the critical values (0.6 to 0.73) for sample sizes of 40 (and 120 for the full sample) (Table 1, Lisle 1985). Passing this  $I_{\text{sym}}$  test indicates a more likely chance that no original fabric was present in the original rock, and further analysis can continue directly towards finding an  $R_s$  value without any need for further manipulation.

Table 2.  $I_{\text{sym}}$  data for sample 6, 7 and 11. These values surpass the critical values given by Lisle (1985) indicating that the rocks had no original fabric prior to deformation

Sample	$I_{\text{sym}}$
6A	0.75
6B	1.3
6C	0.615
7A	0.90
7B	1.23
7C	0.974
11A	0.95
11B	1.05
11C	0.833

$R_f/\Phi$  plots were then constructed. The combined  $R_f/\Phi$  plots containing all data points are shown in Figure 6a, b, c for each face: A, B and C. The values for each individual sample are listed in Table 3. Averaging these data, final strain ratios were determined to be A:1.9, B:2.0, and C:1.5 (All the  $R_f/\Phi$  hard data can be found in the Appendix, along with all other  $R_s$  plots not presented here).

Table 3. Final  $R_s$  values for the three samples and their combined total. As seen, this method is consistent throughout the samples.

Sample	Slide	$R_s$
6	A	1.8
	B	2
	C	1.5
7	A	1.9
	B	2.2
	C	1.7
11	A	1.7
	B	1.9
	C	1.6
Combined	A	1.9
	B	2.0
	C	1.5

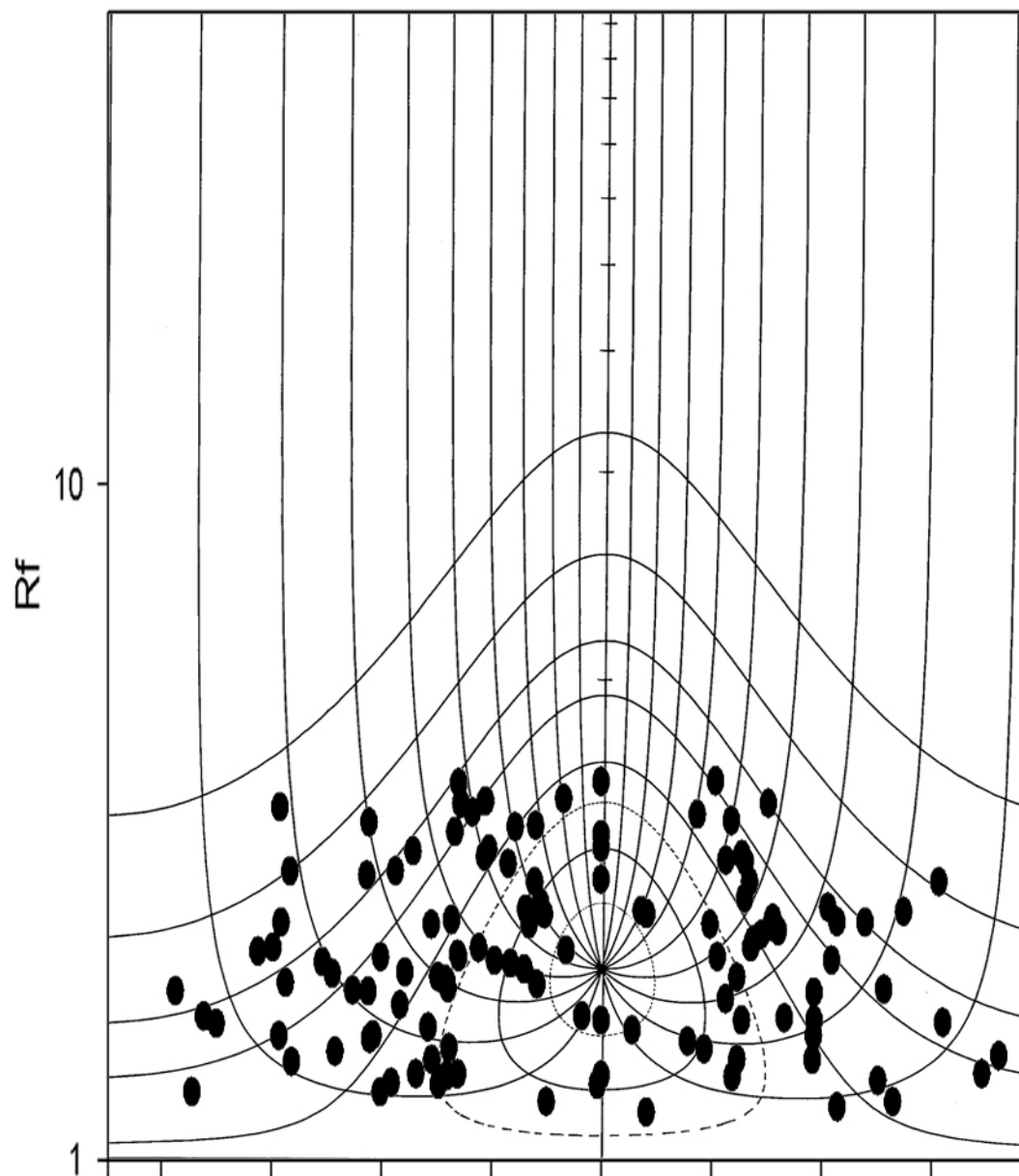


Figure 6a.  $R_s$  plot of the combined data for face A of samples 6, 7 and 11. The average  $R_s$  value is 1.9. The horizontal axis is  $\Phi$  in increments of 20 degrees

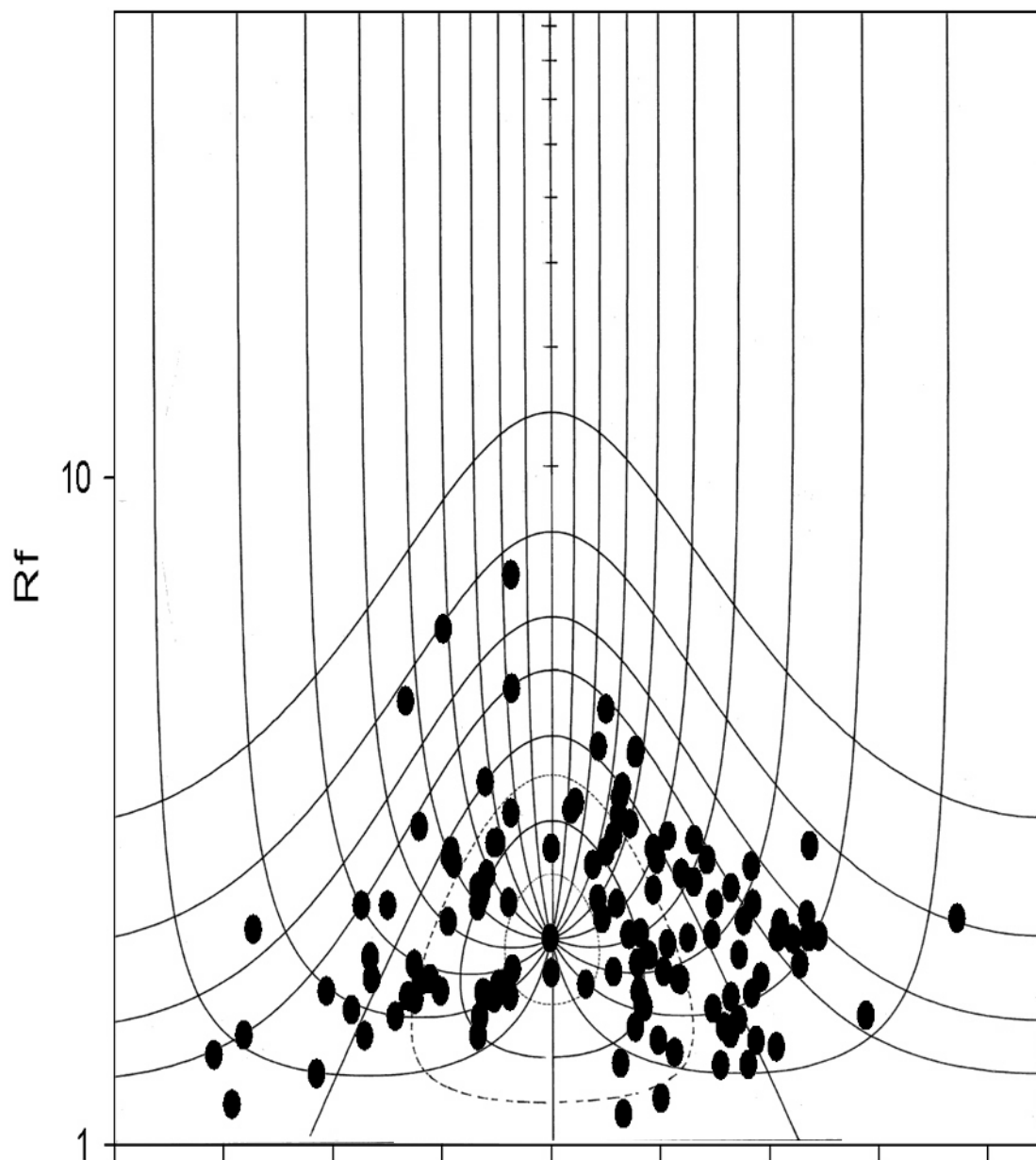


Figure 6b.  $R_s$  plot of the combined data for face B of samples 6, 7 and 11. The average  $R_s$  value is 2.0. The horizontal axis is  $\Phi$  in increments of 20 degrees



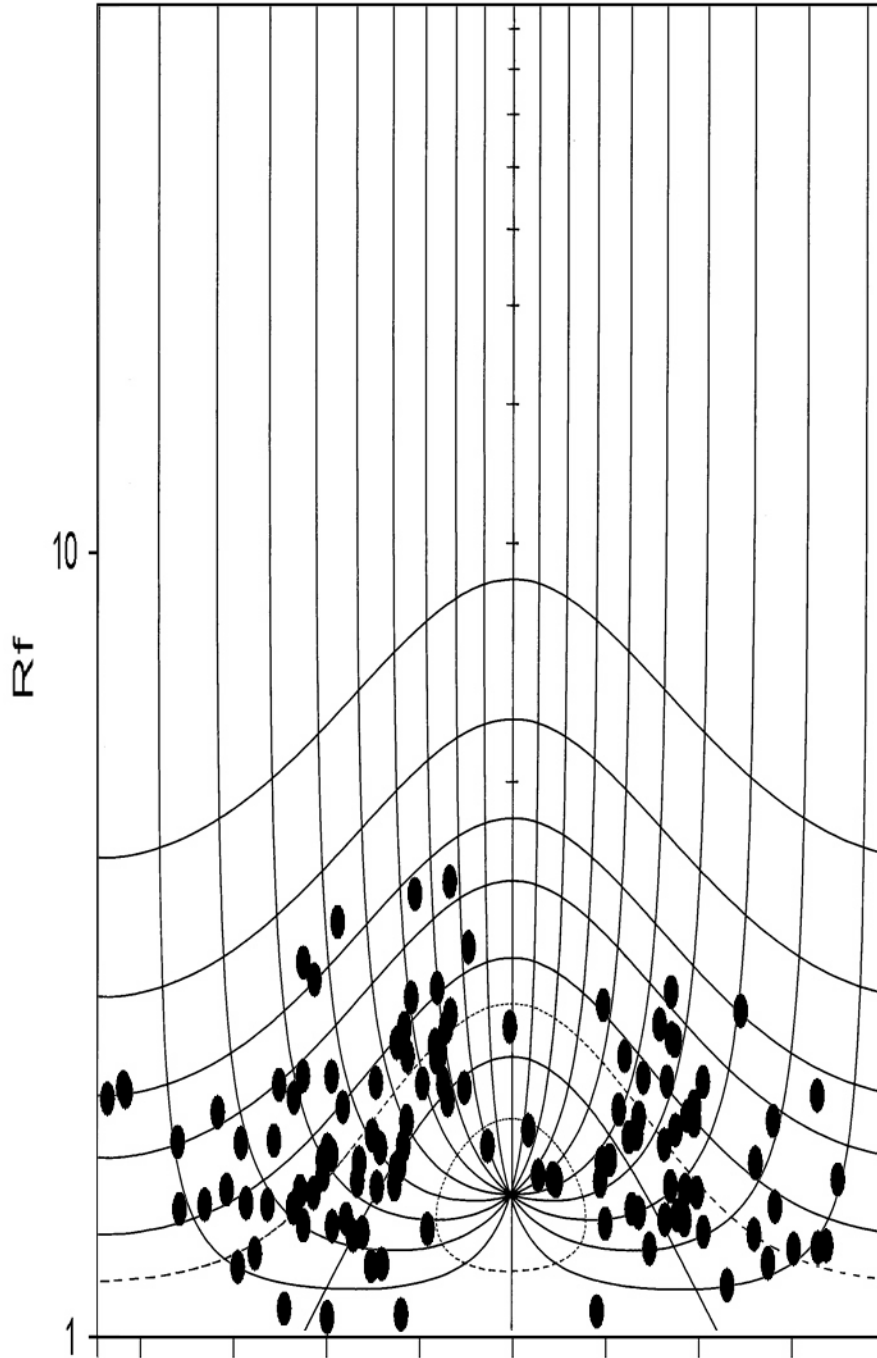


Figure 6c.  $R_s$  plot of the combined data for face C of samples 6, 7 and 11. The average  $R_s$  value is 1.5. The horizontal axis is  $\Phi$  in increments of 20 degrees

## Discussion

Based on strain ratios as determined, A: 1.9, B: 2.0, and C: 1.5, the strain ellipse for these rocks is therefore oriented such that  $S_1$ : B,  $S_2$ : A, and  $S_3$ : C. A Flinn diagram was constructed (Fig. 7). This pattern suggests deformation is mainly plane strain, with perhaps some flattening. This flattening is in the plane of  $S_2$  foliation, as might be expected, and indicates a correlation between the strain in these rocks and the  $D_2$  deformational event of the Horn area. That  $S_1$ , though weak, is in the vertical plane is also consistent with the steeply plunging fold axes of  $F_2$ .

Because these measurements were done with quartz grains, which are fairly resistant, the amount of strain attributed to the Virginia Horn area based on this data is most likely on the low end of a possible range of values. More pronounced strain is evident in other clasts, especially volcanic rock fragments, but it was difficult to make out individual grain boundaries due to alteration effects. Should it become possible to measure these grains, more pronounced  $R_s$  values will likely result.

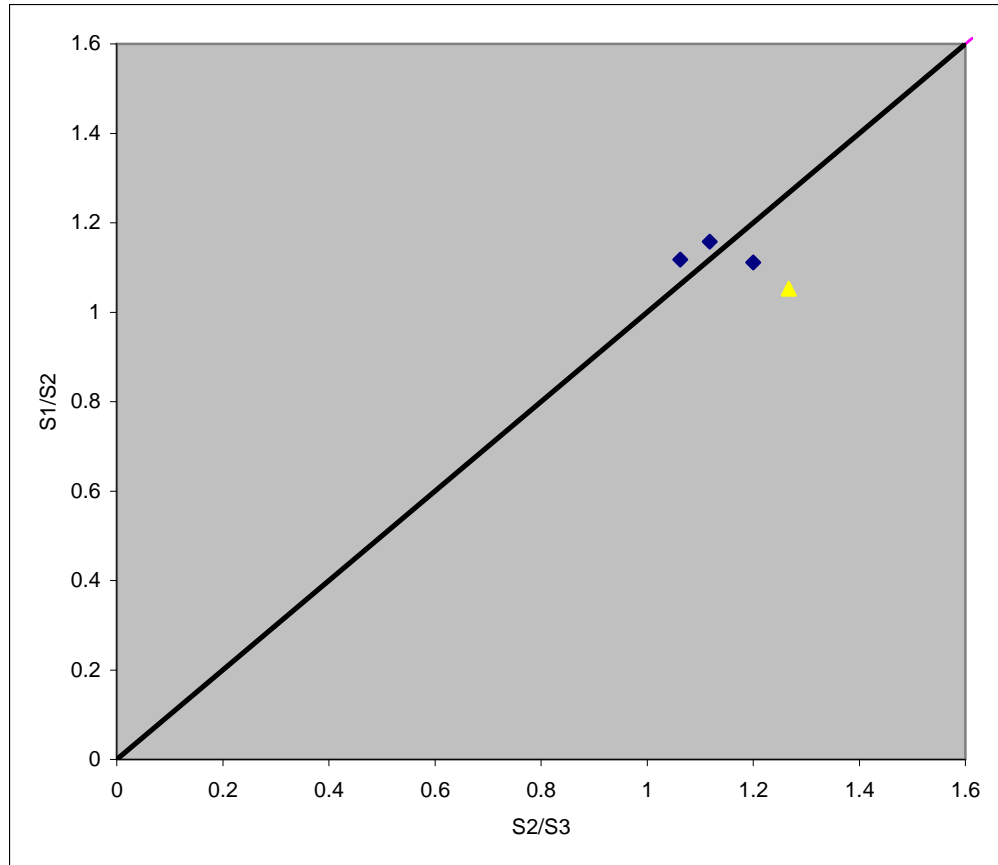


Figure 7. Flinn diagram of the strain ellipse for the samples taken, and a combined sample. All plot closely to the plain strain line, far enough along the x-axis to show a degree of flattening within the plane of cleavage.

### Future Work

Future work for this project would include applying this method of strain analysis to more samples. Likewise, this method of analysis could be extended to the conglomerates of the area, to see if any difference in strain history is present. Similarly, this method could be extended to rocks from the shear zones, as these rocks are likely to show a different strain history.

Performing this method on different clasts might also yield more information. This study was done on quartz grains as they are easier to distinguish amongst the other clasts. It is however quite obvious looking at the thin sections that more deformation can be seen in

the volcanic clasts making up the matrix. A study of these could present a more pronounced strain value.

## Conclusion

The data produced for the three samples were fairly consistent, indicating reliability of the method when applied to rocks from the Virginia Horn. The  $R_s$  values were generally around 1.9, 2, and 1.5 for faces A, B and C respectively, and indicate orientation of the strain ellipse as  $S_1$ : B,  $S_2$ : A, and  $S_3$ : C.

These values show evidence of plane strain, where the  $S_1$  and  $S_2$  axes of the strain ellipse are about equal, and both are slightly larger than  $S_3$ . These two longer axes lie within the plane of foliation. This indicates degree of flattening within the plane of cleavage ( $S_2$ ), consistent with development during  $D_2$  deformation.

## Appendix 1: $R_f/\Phi$ data

Sample	Rf A	Phi A	Rf B	Phi B	Rf C	Phi C
6	1.30	-38.2	1.11	13.2	1.47	-66.2
	1.63	-72.3	1.87	15.8	1.46	-47.2
	2.00	21.1	1.83	-7.1	2.10	-14.9
	1.79	51.4	1.56	-28.6	1.24	-28.1
	2.19	32.2	1.63	16.6	1.43	35.5
	1.26	-40.2	2.34	8.5	1.06	-39.9
	2.68	-37.4	3.14	-7.4	3.14	-9.5
	1.79	-45.2	1.69	-12.5	1.88	-22.8
	1.61	0	2.28	-13.5	2.11	33.2
	2.64	-42.6	1.32	31	1.53	39.6
	3.62	-25.9	2.63	7.6	1.54	-61.5
	1.33	-28.1	1.46	-13.4	1.73	-39.8
	2.00	-25.9	1.67	-7.6	1.76	32.6
	3.06	-26.6	1.18	20.1	1.29	29.4
	2.68	-56.6	1.43	19.6	1.39	19.9
	3.04	0	2.64	-17.9	1.96	-36.5
	2.58	61.4	4.50	10	1.58	9.3
	2.61	0	3.18	3.6	2.60	49
	2.05	-6.4	2.75	10	1.41	32.7
	3.43	-6.8	3.95	8.6	2.00	-14
	1.22	-10	1.87	45.5	1.81	-30.2
	1.34	0	1.38	22.6	1.76	-58.4

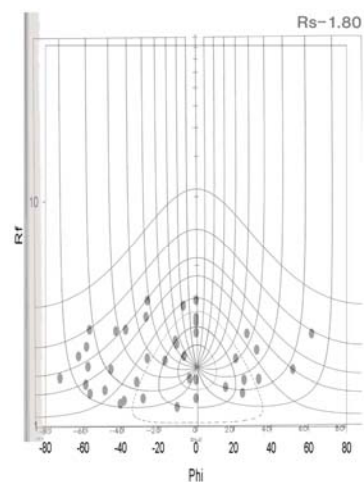
7	2.91	0	2.86	26.2	1.74	-28.5
	1.83	-57.4	2.07	14.2	3.38	-37.6
	1.96	-16.5	2.10	-54.6	1.52	-42.8
	1.61	25.5	1.60	29.6	1.75	-5.4
	2.25	-58.2	1.70	16.1	1.07	-24
	1.63	33.3	2.06	49	1.29	60.4
	1.50	15.7	1.81	0	1.70	-39
	1.53	-58.6	2.05	41.4	2.15	-45.1
	2.40	-11	1.28	-43	1.41	-35.8
	1.58	-31.5	1.77	23.7	1.54	37.1
	1.45	-48.4	1.77	-22.2	1.64	-25.1
	1.64	-3.5	2.00	21.3	2.30	-15.6
	1.41	24.7	2.05	47.1	1.56	-25.4
	2.32	-10.3	2.18	9.3	3.80	-13.5
	2.58	27	1.50	15.4	2.27	-16.4
	1.40	-56.3	2.30	36.9	1.36	41
	3.64	0	1.56	-13.1	1.23	-30.4
	2.04	-62.4	2.31	-7.8	2.15	-38.9
	2.12	27.7	2.68	28.5	2.05	-83.2
	1.46	18.7	3.86	15.4	1.34	-34.3
	2.22	30.8	2.43	32.9	1.78	-51.3
	1.60	62.1	2.81	47.3	3.67	-21
	3.17	-42.2	1.46	-56.3	1.46	56.4
	2.82	-21.2	2.62	36.6	1.60	5.5
	2.77	26.2	3.00	-24.2	1.77	-72
	2.07	-59.7	5.94	-19.8	2.37	-24.9
	1.87	-29.7	2.78	18.7	1.65	-24.4
	1.83	-28	1.67	32.9	2.75	34.1
	2.78	22.7	3.43	13	1.68	-40.8
	1.33	23.8	3.32	12.5	2.57	-13.4
	3.12	-15.6	4.83	-7.3	1.56	33.9
	1.60	-70	3.90	15.5	2.48	-0.6
	2.24	19.8	1.46	-34.2	2.03	65.5
	1.53	-41.5	2.91	21.3	1.44	27.1
	2.24	-30.9	1.92	17.9	2.71	-21.8
	3.33	-58.4	1.79	38.4	2.28	24.1
	1.31	50.3	2.43	-13.4	1.75	-23.5
	2.07	27.2	2.30	29.9	1.36	-32.3
	1.97	-50.7	2.19	74.3	2.08	-83.7
	2.27	-27.2	2.54	-11.8	1.53	-45.7
	1.92	-14	4.63	-26.7	1.38	-38.8
	2.06	-22.3	2.21	46.8	2.65	19.5
	1.78	-77.4	2.76	-18.4	1.66	52.2
	2.88	-20.4	1.15	-58.5	2.50	31.6
	2.25	48	1.74	-9.6	1.59	69.9
	3.64	20.8	1.32	36.1	3.00	-45
	3.28	-23.4	2.84	-10	1.16	46.1

	1.30	-29.6	1.93	34.4	1.67	52.2
	2.32	8.3	3.13	12.3	2.40	34.2
	1.73	22.6	1.54	34.3	1.09	-49.1
	3.18	23.7	1.67	-26.3	2.27	-22.6
	2.33	55	2.30	12	1.83	35
	2.58	-12.1	2.17	35.2	1.67	19.2
	1.56	5.6	1.69	36.7	1.61	-40.8
	1.82	-11.7	2.04	25	1.45	25.6
	2.35	-13.7	2.68	19.3	2.38	34.9
	2.24	-13.1	7.15	-7.4	1.97	39
	2.37	41.2	1.91	-33.2	1.91	37.6
	1.87	24.7	1.33	12.7	2.09	-50.2
	2.87	-34.2	1.65	-25	2.01	-87.1
	1.41	38.4	2.29	-30	1.68	20.9
	2.25	42.9	2.70	-18.7	1.88	56
	3.38	-25.5	1.74	6.3	1.45	-71.6
	2.44	26.1	2.16	-18.9	1.41	36.9
	1.43	72.3	1.77	23.3	1.35	51.9
	2.75	-16.9	2.15	41.9	2.48	-14.3
	1.89	-48.9	3.26	4.4	1.58	-33.4
	3.25	17.5	2.48	26.1	1.88	39
	1.26	-74.4	2.41	18.7	2.02	-47
	1.52	-42.1	1.77	-32.9	2.08	-10.4
	1.18	8.2	1.47	32.8	1.30	65.6
	3.38	30.4	2.55	23.8	2.47	-23.3
	1.29	-0.7	1.43	37.5	1.31	67.4
11	1.41	-30.8	1.70	-20.3	2.85	-42.6
	1.85	-28.4	2.83	-10.5	2.10	-19.4
	1.53	38.6	1.50	31.7	1.67	-33
	1.34	-33.7	1.86	-25.1	1.24	54.9
	1.80	-27.9	2.38	-12.8	1.55	-29.2
	1.34	69.2	1.56	57.6	1.28	-55.4
	2.34	7.3	1.59	-36.6	1.47	-52.7
	1.98	-19.4	3.50	-12.1	1.93	-63.4
	2.02	-26.1	2.78	0	2.11	-29.4
	1.22	53	1.61	17	1.58	18.8
	2.83	25.6	2.89	11.4	1.95	22.8
	1.20	42.9	1.70	-9.9	1.79	25
	3.13	-11.9	1.82	20.6	1.08	18.1
	1.70	-36.6	1.66	-10.5	1.48	-57.3
	3.40	-21	1.70	-41.2	2.35	-16.7
	1.90	-35.7	2.08	16.3	2.14	28.1
	1.78	-42.4	1.82	11.4	1.90	27.1
	2.16	29.1	1.40	41.2	1.23	-59.1
	1.98	41.9	1.76	-24	1.83	3.4
	1.61	38.7	2.07	29.4	2.11	40.9
	1.77	38.7	1.36	-61.8	1.59	8.6

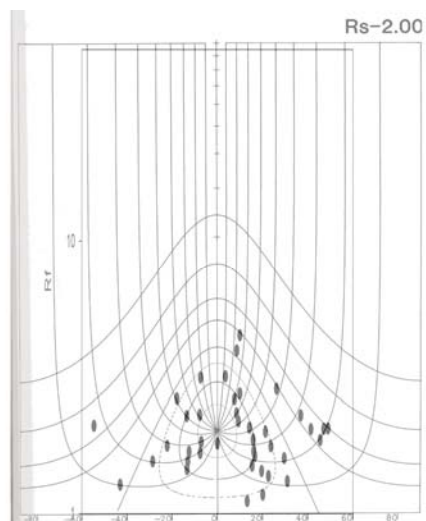
	2.00	-40.1	2.04	44.2	1.37	-18.3
	2.28	31.2	2.04	-0.2	1.38	-45
	1.47	-27.7	3.03	14.4	1.81	26.6
	1.34	-26.1	2.29	-34.8	2.78	-16.2

**Appendix II: R<sub>s</sub> Plots for samples 6, 7 and 11 (following page)**

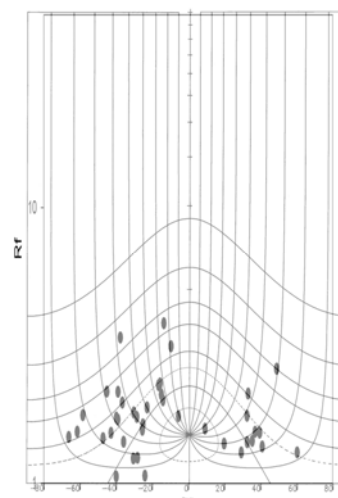
**A**



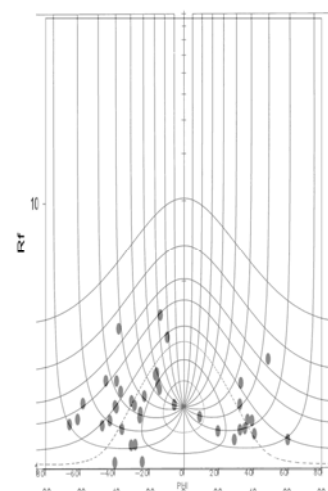
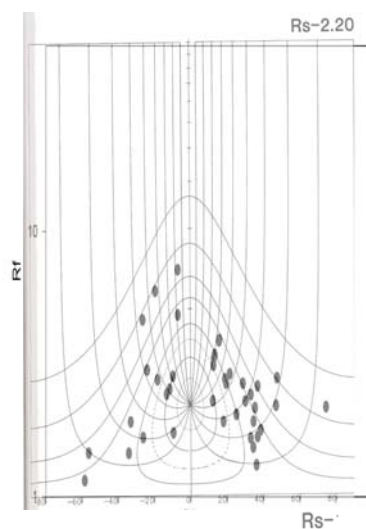
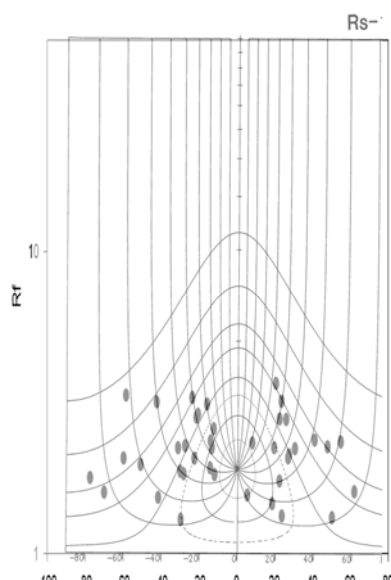
**B**



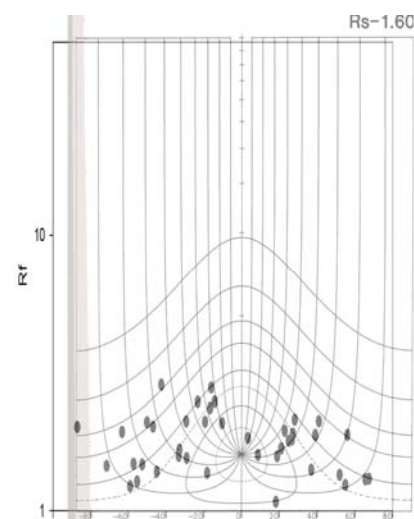
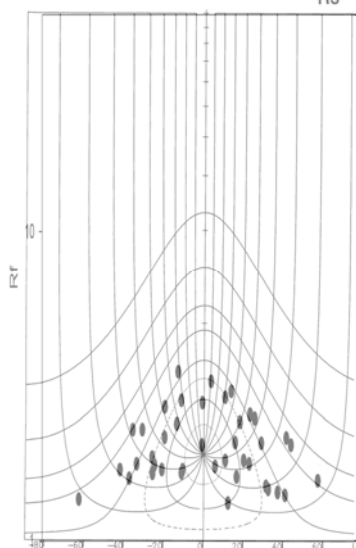
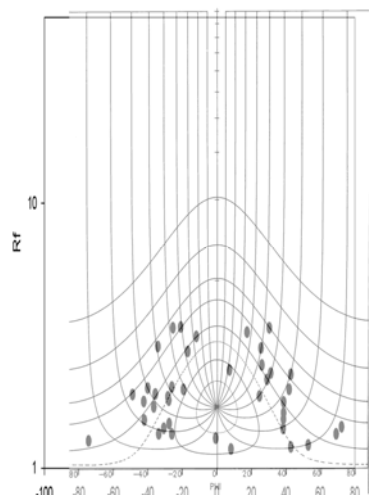
**C**



**6**



**7**



**11**



## References

- Dunnet, D., 1969, A technique of finite strain analysis using elliptical particles: *Tectonophysics*, v. 7, p. 117-136.
- Jirsa, M.A., and Boerboom, T.J., 2003, Geology and mineralization of Archean bedrock in the Virginia Horn: Contribution to the geology of the Virginia Horn Area, St. Louis County, Minnesota, Jirsa, M.A., and Morey, G.B. eds., p. 10-10-73.
- Jirsa, M.A., Boerboom, T.J., and Morey, G.B. 1998, Bedrock geologic map of the Virginia Horn Mesabi Iron Range, St. Louis County, Minnesota: Minnesota Geological Survey Miscellaneous Map M-85, scale 1:48,000.
- Lisle, Richard J., 1985, Geological Strain Analysis, A Manual for the  $R_f/\phi$  Technique: Great Britain, Pergamon Press.
- Ramsay, J.G., 1967, Folding and Fracturing of Rocks, McGraw-Hill, New York.
- Sutton, T.C. 1963, Geology of the Virginia Horn Area. Minneapolis, University of Minnesota, M.S. thesis, 97 p., 5 pls.
- Welsh, J.L. 1989. Strike-slip faulting in Archean rocks in the Virginia Horn area, N.E. Minnesota: Implications for the origin of the Virginia Horn structure [abs.]: Institute on Lake Superior Geology, 35<sup>th</sup> Annual Meeting, Duluth, Minn., Proceedings and Abstracts, v. 35, pt. 1, p. 101.
- Welsh, J.L., England, D.L., Groves, D.A., Levy, E., 1989, General Geology and the Structure of Archean Rocks of the Virginia Horn Area, Northeastern Minnesota: Institute on Lake Superior Geology Proceedings Part 2: field trip guidebook, v. 35, p. D 1-9.
- Welsh, J.L., Englebert, J.A., and Hauck, S.A., 1991, General Geology, Structure, and Geochemistry of Archean Rocks of the Virginia Horn Area, Northeastern Minnesota: Bedrock Geochemistry of Archean Rocks in Northern Minnesota, Center for Applied Research and Technology Development, Natural Resources Research Institute, University of Minnesota, Duluth, Englebert, J.A. and Hauck, S.A eds., p. 100-137.